

Electronic Structure and Lattice Dynamics in the FeSb₃ Skutterudite from Density Functional Theory

Mikael Råsander,^{1,*} Lars Bergqvist,^{1,2} and Anna Delin^{1,2,3}

¹*Department of Materials and Nanophysics, KTH Royal Institute of Technology, Electrum 229, SE-164 40 Kista, Sweden*

²*SeRC (Swedish e-Science Research Center), KTH, SE-100 44 Stockholm, Sweden*

³*Department of Physics and Astronomy, Uppsala University, Box 516, SE-751 20 Uppsala, Sweden*

(Dated: February 15, 2022)

We have performed density functional calculations of the electronic structure and lattice dynamics of the binary skutterudite FeSb₃. We find that the ground state of FeSb₃ is a near semi-metallic ferromagnet with $T_c = 175$ K. Furthermore, we find that FeSb₃ is softer than CoSb₃ based on an analysis of the relation of the elastic constants and the shape of the phonon density of states in the two systems, which is in agreement with experimental observation. Based on these observations we find it plausible that FeSb₃ will have a lower thermal conductivity than CoSb₃. Additionally, our calculations indicate that FeSb₃ may be stable towards decomposition into FeSb₂ and Sb. Furthermore, for ferromagnetic FeSb₃ we obtain real-valued phonon frequencies and also a c_{44} greater than zero, indicating that the system is mechanically as well as dynamically stable.

I. INTRODUCTION

The skutterudites constitute an interesting class of materials for applications as thermoelectric energy converters,¹ since they possess the necessary electronic properties, notably a large Seebeck coefficient, and a low thermal conductivity. The latter is largely due to filler atoms that occupy large voids in the crystal structure.²⁻⁶ The exact mechanism of the filler atoms to lower the thermal conductivity is however debated.⁷ The skutterudites can generally be presented as $R_yM_4X_{12}$, where M is a transition metal, such as Co, Ir, Rh. X is a pnictogen, e.g. P, As and Sb, and R is the filler atom, typically a rare earth element, such as La or Ce. The skutterudites offer a rich ability for engineering in order to optimize their properties by alloying on the metal or pnictogen lattices, as well as by careful selection of the filler element.

CoSb₃ is an archetypical skutterudite system. It has excellent electronic properties and especially it has a high Seebeck coefficient.⁸⁻¹⁰ Unfortunately, the thermal conductivity of CoSb₃ is too large for achieving a high thermoelectric efficiency. The ability to lower the thermal conductivity in CoSb₃ by using filler atoms is limited¹¹ since the filling factor, y , is rather small and focus on filled skutterudites has been directed towards other skutterudites, such as Fe containing $R_yFe_xCo_{1-x}Sb_{12}$ since the filling factor is larger for such systems and for $R_yFe_4Sb_{12}$ the filling factor reaches unity.²⁻⁶ Filled $R_yFe_4Sb_{12}$ systems have been studied for quite some time. However, the binary FeSb₃ system has not received much attention even though an understanding of the dynamics of the filler and its impact on the electronic structure and thermal conductivity cannot be complete without an understanding of the properties of the host framework. According to the phase diagram¹² FeSb₃ is metastable in comparison to FeSb₂, which also possess interesting thermoelectric properties, and Sb. Recently, however, micrometer thick films of FeSb₃ has been synthesized by nanoalloying of Fe and Sb precursors at

$T \sim 400$ K^{13,14} and its physical properties investigated experimentally.¹⁴ A significant difference compared to CoSb₃ is that FeSb₃ is softer and a softening of low-energy phonon modes would likely have a favorable influence towards a lower thermal conductivity of FeSb₃ compared to CoSb₃.

Since there are no theoretical studies focusing on FeSb₃ we investigate the electronic structure, lattice dynamics and possible dynamic stability of FeSb₃ using methods based on density functional theory. We compare our results with calculations for the well-known CoSb₃ system in order to elucidate the differences between these two superficially rather similar compounds. In addition, we will analyze how filling the voids in FeSb₃ with La affects the lattice dynamics.

The paper is outlined as follows: In Section II we will present the details of our calculations and in Section III we will present our results. Finally in Section IV we will summarize our findings and present our conclusions.

II. COMPUTATIONAL DETAILS

The binary skutterudite structure has a unit cell containing four formula units with body centered cubic lattice vectors and belongs to the space group Im-3 (No. 204), where metal atoms and pnictogen atoms occupy the $8c$ and $24g$ positions respectively. The Sb atoms occupy the general position $(0,y,z)$ and these values along with our calculated lattice constants are shown in Table I. The skutterudite framework, i.e. MX_3 , contains large voids at the $2a$ positions of the lattice. Filling these voids by other atoms do not change the symmetry of the crystal. In Fig. 1 we show the conventional unit cell of the skutterudite structure (8 formula units) with the voids, at $(0,0,0)$ and $(\frac{1}{2},\frac{1}{2},\frac{1}{2})$, filled with a rare-earth element. In this study the rare-earth element is La, and calculations have been performed for FeSb₃ and CoSb₃ binary skutterudite and the filled LaFe₄Sb₁₂.

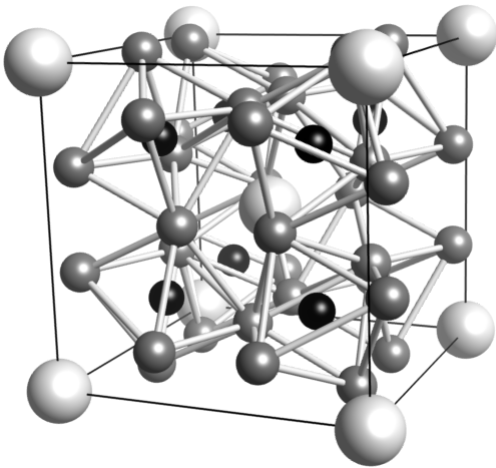


FIG. 1. Illustration of the crystal structure of the skutterudite structure. Fe (black spheres) is residing inside canted octahedral cages of Sb (grey spheres). Filler atoms are presented by large white spheres. In this case the filler is La.

Density functional calculations have been performed using the projector augmented wave (PAW) method¹⁵ as it is implemented in the Vienna *ab-initio* simulation package (VASP)^{16,17}. The generalized gradient approximation due to Perdew, Burke and Ernzerhof (PBE)¹⁸ has been used for the exchange-correlation energy functional. Relaxation of the ionic position as well as the volume of the systems have been performed until the forces on individual atoms were smaller than 0.1 meV/Å. A k-point mesh of $6 \times 6 \times 6$ ¹⁹ was found to be accurate enough for obtaining converged total energies and structural parameters. The plane wave energy cut-off was set to 600 eV. Spin-polarization was considered for all systems and it will be made clear when a non spin-polarized (NSP), ferromagnetic (FM) or anti-ferromagnetic (AFM) solution is discussed. Here, we focus on the electronic structure and lattice dynamics of the FeSb₃ system in relation to the more studied CoSb₃ and LaFe₄Sb₁₂ systems and a more elaborate study of the magnetic properties of FeSb₃ will be published elsewhere in conjunction with Co_{1-x}Fe_xSb₃ alloyed systems.²⁴ However, here we have accurately calculated the Curie temperature (T_c) of FeSb₃ by calculating the exchange parameters within a Heisenberg model using the SPR-KKR package,²⁰ where the crystal geometry was taken from our PAW calculations, and subsequent Monte Carlo simulations using the UppASD package.²¹ We have also checked the effects of spin-orbit coupling on the electronic structure and lattice dynamics in FeSb₃ and CoSb₃ and found that the effects are rather minor.

The lattice dynamics have been calculated within the harmonic approximation at $T = 0$ K by means of the small displacement method, as it is implemented in the Phonopy code.²² The results shown here are obtained for a $3 \times 3 \times 3$ multiplication of the primitive skutterudite

TABLE I. Comparison of the evaluated lattice constants and crystallographic y and z values for the Sb atoms in FeSb₃ for spin-polarized (in ferromagnetic (FM) and anti-ferromagnetic (AFM) configurations) and non spin-polarized (NSP) calculations.

System		a (Å)	y	z
FeSb ₃	NSP	9.153	0.327	0.160
FeSb ₃	FM	9.178	0.331	0.160
FeSb ₃	AFM	9.166	0.331	0.159
FeSb ₃	exp ¹³	9.176	0.340	0.162
FeSb ₃	exp $T = 10$ K ¹⁴	9.212	0.340	0.158
FeSb ₃	exp $T = 300$ K ¹⁴	9.238	0.340	0.157
CoSb ₃	NSP	9.115	0.333	0.160
CoSb ₃	exp ²³	9.039	0.335	0.158
LaFe ₄ Sb ₁₂	NSP	9.181	0.335	0.164
LaFe ₄ Sb ₁₂	FM	9.186	0.335	0.163

unit cell which is considered large enough to yield well converged lattice dynamical properties. The size of the displacements were 0.01 Å. For the supercells a $2 \times 2 \times 2$ k-points mesh has been used for the electronic structure calculations from which the forces acting on the atoms have been evaluated. In the calculations of the phonon density of states (PDOS) a $20 \times 20 \times 20$ q-points mesh has been utilized.

III. RESULTS

A. Structural properties and phase stability

In Table I we show the evaluated structural parameters for FeSb₃, CoSb₃ and LaFe₄Sb₁₂. We find that the non spin-polarized (NSP) calculation for FeSb₃ yield a smaller lattice constant compared to the result obtained by ferromagnetic (FM) and anti-ferromagnetic (AFM) calculations. The y and z coordinates are however similar in all three cases, especially so for the z coordinate. Compared to experiments there is a very good agreement in the lattice constant between the FM calculation and the experiment by Hornbostel et al.¹³, while the lattice constant obtained by Möchel et al.¹⁴ is much larger compared to our theoretical results. Both of the experimental studies on FeSb₃ also find $y = 0.340$ which is larger than our value of 0.331. However, the z values are very similar. Compared to CoSb₃ the Fe containing system has a larger lattice constant, while the y and z values are very similar in our calculations. When filling the voids in FeSb₃ with La, we find that the lattice constant increases by ~ 0.03 Å in the case of NSP calculations and by ~ 0.01 Å in the case of FM calculations, which means that incorporation of La into the lattice is made easier for the FM system.

In addition, we have calculated the energy of the FeSb₃ phase in relation to FeSb₂ and elemental Sb according to

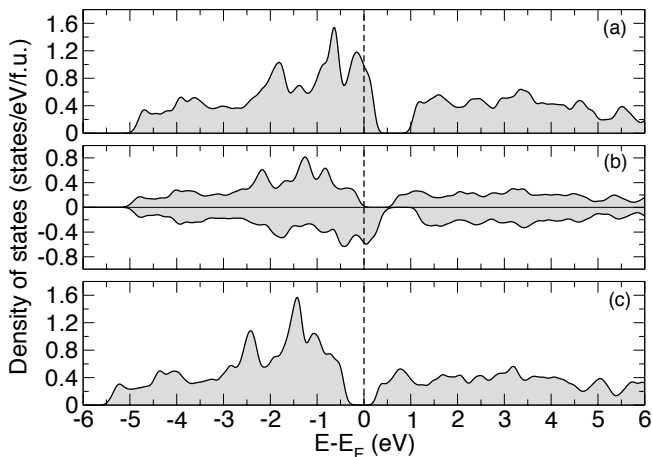


FIG. 2. Calculated density of states (DOS) of the upper valence and lower conduction band regions of (a) NSP FeSb₃, (b) FM FeSb₃ and (c) CoSb₃. In (b) the positive DOS are for the spin-up channel and the negative valued DOS are for the spin-down channel. The vertical dashed lines mark the position of the Fermi level.

$\Delta E = E(\text{FeSb}_3) - E(\text{FeSb}_2) - E(\text{Sb})$, where $E(X)$ is the total energy of system X with $X = \text{FeSb}_3, \text{FeSb}_2$ and Sb. Here, FeSb₂ has been evaluated in its orthorhombic ground state with the space group Pnn2, while Sb has been calculated in the A7 trigonal structure with space group R3-mh. For these calculations, we have also increased the density of the k-points mesh to $12 \times 12 \times 12$ for FeSb₃ and FeSb₂. For Sb the mesh was set to $12 \times 12 \times 6$. The resulting very small energy difference of -0.02 eV/f.u. suggests that the FeSb₃ phase may be stable or nearly stable towards decomposition into FeSb₂ and elemental Sb. We note that if SOC is included $\Delta E = -0.01$ eV/f.u. Note that these energies are normalized per formula unit, f.u., of FeSb₃.

B. Electronic structure

In Fig. 2 we show the electronic density of states (DOS) of NSP FeSb₃, FM FeSb₃ and CoSb₃. It is clear that NSP FeSb₃ is a metal with a large DOS at the Fermi level, E_F . The DOS also contains a gap between the valence band edge and higher lying conduction bands. Furthermore, the electronic properties FeSb₃ is very different from CoSb₃, which is a semiconductor with a small direct gap at the Γ point of about 0.2 eV in agreement with previous theory.⁹ The large DOS at the Fermi level in the NSP FeSb₃ makes it energetically favorable for the system to form a ferromagnetic ground state, which can be deduced from the Stoner criterion, i.e. $N(E_F)I > 1$, where $N(E_F)$ is the DOS at the Fermi level and I is the Stoner exchange parameter. FM FeSb₃ can be described as a near half-metal, where the spin up channel is almost completely filled with a direct gap at the Γ point of about 0.3 eV. The spin down channel has a significant DOS at

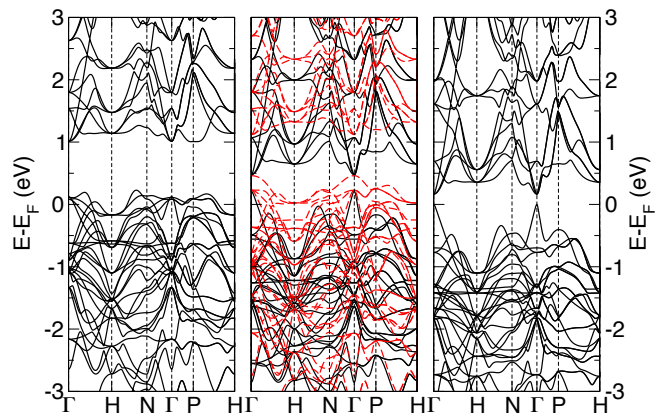


FIG. 3. (Color online) Calculated band structures along high symmetry directions in the Brillouin zone of NSP FeSb₃ (left panel), FM FeSb₃ (middle panel) and CoSb₃ (right panel). In the middle panel the spin-up bands are plotted with solid (black) lines and the spin-down bands are plotted with dashed (red) lines. The zero on the energy scale is the Fermi level, E_F .

the Fermi level and up to about 0.5 eV above the Fermi level when a gap of about 0.7 eV is found to the higher lying conduction bands.

The magnetic moments in the FM and AFM calculations is to a great extent localized on the Fe atoms, with a magnetic moment of $\sim 1.0 \mu_B/\text{Fe}$ and $\sim 1.1 \mu_B/\text{Fe}$ respectively. The same is also true for FM LaFe₄Sb₁₂, however, for this system the magnetic moment on the Fe has dropped to $\sim 0.3 \mu_B/\text{Fe}$. We also find small induced moments on the Sb atoms (less than $0.01 \mu_B/\text{atom}$) and on the La ($\sim 0.05 \mu_B$) in the opposite direction to the moments localized on the Fe atoms. The magnetization energy, i.e. the energy between the FM (or AFM) and the NSP calculations, is for FeSb₃ -0.28 eV (FM) and -0.13 eV (AFM), which shows that FM FeSb₃ is the ground state. For this ground state, we obtained a Curie temperature of 175 K which is well below the relevant thermoelectric operating temperatures. In the case of LaFe₄Sb₁₂ the magnetization energy has been lowered to -0.02 eV which is very small and throughout the remainder of the paper we will only consider NSP LaFe₄Sb₁₂. As expected CoSb₃ shows no tendency for a magnetic solution. A more detailed account of the magnetic properties of FeSb₃ and Fe_xCo_{1-x}Sb₃ alloys will be presented in Ref. 24.

In addition to the calculated DOS we show in Fig. 3 the calculated band structures for the NSP FeSb₃, FM FeSb₃ and CoSb₃. It is clear that the electronic structure of FeSb₃ and CoSb₃ is significantly different: In CoSb₃ the highest valence band sticks out above the other bands at the Γ point with a quadratic dispersion close to Γ that turns into a linear dispersion which extends far out into the Brillouin zone, especially along Γ to H.⁸ This dispersion is also found in FeSb₃ however, for the NSP FeSb₃ this band is coexisting with several bands with small dispersion which give rise to the large DOS at the

TABLE II. Calculated elastic constants of NSP, FM and AFM FeSb₃ in comparison to CoSb₃ calculated according to Refs. 26 and 27. $B = (1/3)(c_{11} + 2c_{12})$ is the bulk modulus and $c' = (1/2)(c_{11} - c_{12})$ is the tetragonal shear constant.

System	c_{11} (GPa)	c_{12} (GPa)	c_{44} (GPa)	B (GPa)	c' (GPa)
NSP	166.0	41.7	22.0	83.1	62.2
FM	166.0	37.1	35.0	80.1	64.5
AFM	156.6	37.0	31.6	76.9	59.8
CoSb ₃	181.8	36.5	49.4	84.9	72.7

Fermi level. For FM FeSb₃ the same band is found in the spin up channel, however, here there are several spin down bands at the same energy.

C. Elastic constants and the velocity of sound

In Table II we show the calculated elastic constants of FeSb₃ and CoSb₃. We find that essentially all elastic constants is smaller in FeSb₃ compared to CoSb₃. It is only c_{12} that is larger in FeSb₃, although the differences in the elastic constants in the two systems are small. The bulk modulus B and the tetragonal shear constant c' are both larger in CoSb₃ compared to FeSb₃. We can therefore conclude that the FeSb₃ framework is softer than CoSb₃, which is in agreement with experimental findings¹⁴ as well as with our analysis of the lattice dynamics, see below. Mochel et al.¹⁴ have reported the bulk modulus of FeSb₃ to be 47.9(1) GPa¹⁴ which is much smaller than the values obtained by us here. This could be related to the difference in lattice constant between our calculation and the experiment, see Table I, where the lattice constant of Ref. 14 is larger than the theoretical value. Since the bulk modulus can be expressed as $B = (1/V)\partial^2 E/\partial V^2$, a large difference in the volume will affect the bulk modulus. For CoSb₃ the experimental bulk modulus is 83.2(1) GPa¹⁴ which is in excellent agreement with our result.

The difference in the size of the elastic constants will affect the velocity of sound in the materials, since the velocity of sound in a given direction is given by $c = \sqrt{c_{\text{eff}}/\rho}$, where c_{eff} is a linear combination of elastic constants depending on the direction and ρ is the mass density of the material. A simple analysis yields that the increased stiffness of CoSb₃ compared to FeSb₃ means that sound waves travel more readily in CoSb₃. Since the velocity of sound is in turn related to the thermal conductivity of the material we may anticipate that the thermal conductivity is lower in FeSb₃ compared to CoSb₃. However, this has to be supported in a more rigorous fashion.

D. Lattice dynamics

In Fig. 4 we show the calculated phonon dispersion energies of FeSb₃ obtained from a non spin-polarized

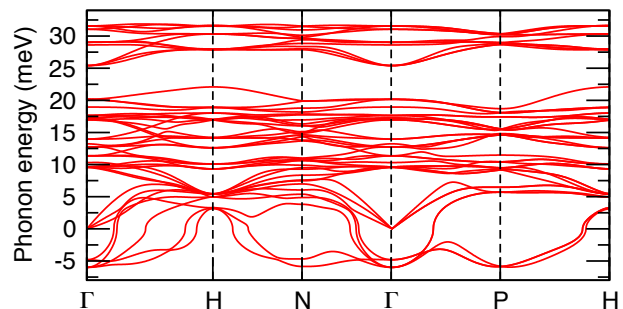


FIG. 4. (Color online) The resulting phonon dispersions along high symmetry directions in the Brillouin zone based on a non spin-polarized density functional calculation of FeSb₃. Imaginary phonon energies are plotted with negative values. Note the imaginary phonon energies along all directions shown.

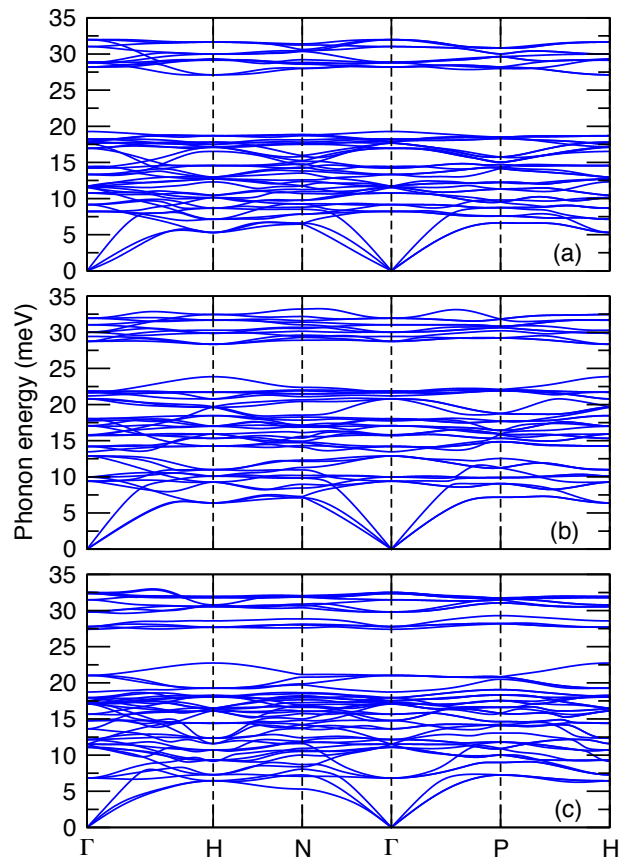


FIG. 5. (Color online) Calculated phonon dispersions for (a) FM FeSb₃, (b) CoSb₃ and (c) LaFe₄Sb₁₂ along high symmetry directions in the Brillouin zone.

(NSP) density functional calculation. Several phonon modes have imaginary phonon energies and it is clear that NSP FeSb₃ is dynamically unstable within the harmonic approximation. By allowing for a FM solution this behavior will change and all phonon modes will have real values. This is shown in Fig. 5, where we present the calculated phonon energies of FM FeSb₃ and compare the

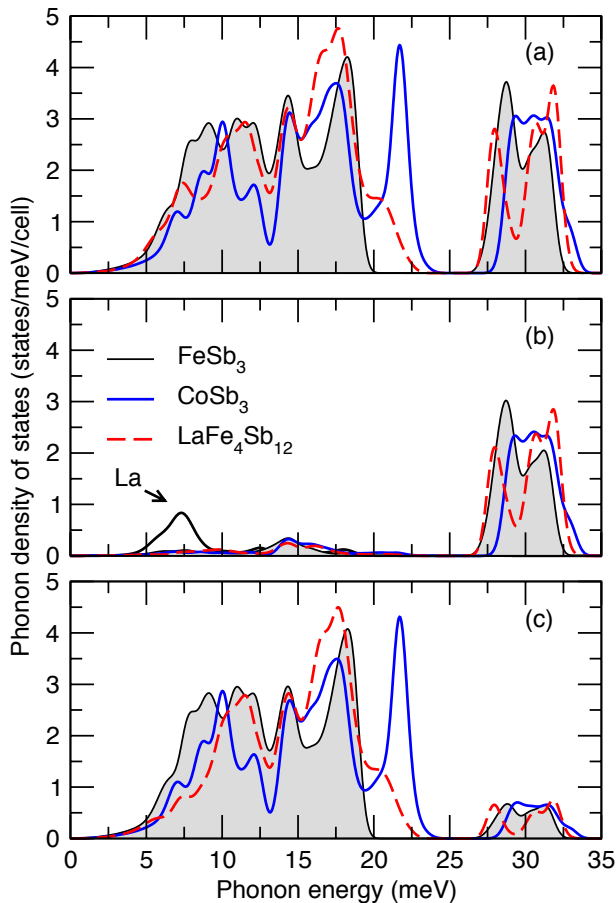


FIG. 6. (Color online) Phonon density of states (PDOS) of FeSb₃, CoSb₃ and LaFe₄Sb₁₂, (a) total PDOS, (b) projected PDOS on metallic species, i.e. Fe, Co and La, (c) projected PDOS on Sb. The projected PDOS onto La is given by the thick black line in (b). For clarity, the PDOS on atoms in the FeSb₃ system are shaded in grey. Note that the unit is states/meV/cell, where the cell is the either Fe₄Sb₁₂, Co₄Sb₁₂ or LaFe₄Sb₁₂.

results with the phonon energy dispersions for CoSb₃ and LaFe₄Sb₁₂. For the remainder of the paper we will focus only on FM FeSb₃ and the FM descriptor will be omitted throughout.

In Fig. 5, it is clear that the phonon modes can be divided into two regions in terms of energy: The lower region which contains both acoustic and optical modes, which in the case of FeSb₃ lies in the energy range of 0 to 20 meV, and the upper optical region, which for FeSb₃ lies in between 27 to 33 meV. In CoSb₃ the lower region reaches ~ 25 meV which is about 5 meV higher in energy compared to FeSb₃. This suggests that FeSb₃ is softer than CoSb₃ which agrees well with recent experimental findings¹⁴. In addition, we find that the upper optical region in LaFe₄Sb₁₂ is split in two regions with a gap at 27 meV, which is dramatically different from the behavior in the binary systems where this region contains modes with dispersions that cross and overlap each other. For CoSb₃ there is a narrow gap at about 13 meV

which splits the lower phonon energy region. Among the systems studied here, this gap is unique to CoSb₃. The existence of this gap has been observed previously by both theory and experiment.²⁻⁶ We also note a clear signature of avoided crossing²⁵ of the acoustic and low lying optical modes in LaFe₄Sb₁₂ along the line connecting Γ to P which does not exist in the binary systems. The acoustic phonon modes are also found to be non degenerate along most directions in the Brillouin zone. It is only along Γ to P where the two lowest energy phonon modes are degenerate for all three systems in our study.

In Fig. 6 we have plotted the total and projected phonon density of states (PDOS) for FeSb₃, CoSb₃ and LaFe₄Sb₁₂. In FeSb₃ the lower energy region between 0 and 20 meV is dominated by Sb and the upper region between 27 to 33 meV is dominated by Fe. We find that the PDOS of Fe has two small broad peaks at ~ 7 meV and ~ 15 meV, as well as a larger feature between 27 and 33 meV which has two clear peaks, see panel (b) in Fig. 6. The Sb projected PDOS is more or less flat between 0 and 20 meV with two valleys at ~ 13 meV and ~ 16 meV. These observations are in good agreement with available experimental PDOS measured by M \ddot{o} chel et al.¹⁴ Compared to CoSb₃, also plotted in Fig 6, the PDOS of FeSb₃ show the same behavior as the phonon dispersions that the lower phonon energy region is narrower in FeSb₃. In addition, in CoSb₃ the Sb projected PDOS shows distinct features, such as two deep valleys at ~ 13 meV and ~ 20 meV as well as a very distinct peak at ~ 22 meV. The very deep valley at 13 meV coincides with the gap in the phonon dispersions for CoSb₃ shown in Fig. 5. The peak at 22 meV and valley at 20 meV mark significant differences to the Sb PDOS in FeSb₃. For the PDOS projected onto Co we find that it also show smaller features at the same energies as the Fe PDOS in FeSb₃, however the feature at large phonon energies is shifted to slightly larger energies for the Co PDOS compared to the case of Fe in FeSb₃, and this feature is flat which is a distinct difference to Fe in FeSb₃. The two binary skutterudite systems therefore show distinct differences in their lattice dynamics and especially so for the dynamics of the Sb atoms in the two systems.

When La is inserted into FeSb₃, we find that the total PDOS from 0 up to about 7.5 meV are very similar, however, when projected onto Sb there is a marked difference between the filled and unfilled systems. The Sb PDOS has been reduced in response to the filling in this region. This reduction in the Sb PDOS for LaFe₄Sb₁₂ coincides with the appearance of a filler mode due to vibrations of the La centered about 7 meV, see Fig. 6. We also find features in the Sb PDOS for the filled system at this energy which suggests that the La and Sb vibrations are connected and not independent which is in agreement with experimental observations⁷. In addition to the large La peak at about 7 meV, we find several small features in the La PDOS at about 12.5 meV and 18 meV in agreement with previous theory and experiment.² Furthermore, we find that the PDOS of the filled system is

broadened compared to the unfilled FeSb₃ and that the Fe PDOS region at high phonon energies are split with a deep valley at just below 30 meV. This latter feature is due to the gap in the high energy optical modes which is clearly visible in Fig. 5.

IV. SUMMARY AND CONCLUSIONS

We have performed density functional calculations on the FeSb₃ skutterudite system and analyzed its electronic structure and lattice dynamics. The electronic structure has been compared in detail with CoSb₃ while for the lattice dynamics comparison has also been done with the filled LaFe₄Sb₁₂ skutterudite phase. We find that FeSb₃ is a near semi-metal with a ferromagnetic ground state and a Curie temperature of 175 K. The non spin-polarized FeSb₃ is a metal with a large DOS at the Fermi level which facilitates the ferromagnetic ground state.

We find that in order to obtain a dynamically stable system it is required to evaluate the lattice dynamics for the ferromagnetic ground state of FeSb₃. Phonon calculations for the non spin-polarized phase yield unstable phonon modes along most high symmetry directions. We note that the calculations of the lattice dynamics have been done within the harmonic approximation at $T = 0$ K. However, the harmonic approximation is known to fail for systems that are stabilized at finite temperatures, since anharmonic effects are not included in the calculation. Famous examples are the high temperature phases of Zr,^{28,29} Ti²⁹ and Hf²⁹ which all have the bcc structure at elevated temperatures even though the bcc structure for these systems is dynamically unstable in the harmonic approximation. The low T_c for FeSb₃ combined with the fact that the phase is made experimen-

tally at ~ 400 K^{13,14} suggest that the non spin-polarized phase will be stabilized at finite temperature in a similar fashion as the examples mentioned above.

Compared to CoSb₃ we find that the lattice dynamics in FeSb₃ differs in several respects, for example: The Sb PDOS in FeSb₃ is more flat and narrower compared to CoSb₃ which shows more features in the PDOS, especially a significant peak about 22 meV that is not present in FeSb₃. In addition, the PDOS of Fe at large phonon energies show a clear two peak feature which is not the case in CoSb₃ which is more flat. We also find that FeSb₃ is softer than CoSb₃ based on the form of the phonon energy dispersions and PDOS as well as from calculations of the elastic constants of the two systems.

When compared to filled LaFe₄Sb₁₂, we find a hardening at low phonon energies for the filled system of the Sb PDOS which coincides with the La PDOS peak centered at 7 meV. This hardening of the Sb PDOS is in perfect agreement with the experimental result of Möchel et al.¹⁴

Furthermore, we find that FeSb₃ is mechanically stable, i.e. have B , c' and c_{44} greater than zero, as well as dynamically stable in its bulk form. This suggests that it should be in principle possible for a process route to be established in order to produce bulk samples of binary FeSb₃.

V. ACKNOWLEDGEMENTS

This work was financed through the EU project Next-Tec, VR (the Swedish Research Council), and SSF (Swedish Foundation for Strategic Research). The computations were performed on resources provided by the Swedish National Infrastructure for Computing (SNIC) at the National Supercomputer Centre in Linköping (NSC).

* mikra@kth.se

¹ G. J. Snyder and E. S. Toberer, *Nature Mater.*, **7**, 105-114 (2008).
² J. L. Feldman, P. Dai, T. Enck, B. C. Sales, D. Mandrus and D. Singh, *Phys. Rev. B* **73**, 014306 (2006).
³ J. L. Feldman and D. J. Singh, *Phys. Rev. B* **53**, 6273 (1996).
⁴ J. L. Feldman and D. J. Singh, *Phys. Rev. B* **54**, 712E (1996).
⁵ R. P. Hermann, R. Jin, W. Schweika, F. Grandjean, D. Mandrus, B. C. Sales and G. J. Long, *Phys. Rev. B* **90**, 135505 (2003).
⁶ C. A. Kendziora and G. S. Nolas, *Mater. Res. Soc. Symp. Proc.* **793**, 107 (2004).
⁷ M. M. Koza, M. R. Johnson, R. Viennois, H. Mutka, L. Girard and D. Ravot, *Nature Mater.* **7** 805-810 (2008).
⁸ J. C. Smith, S. Banerjee, V. Pardo and W. E. Pickett, *Phys. Rev. Lett.* **106** 056401 (2011).
⁹ D. Wee, B. Kozinsky, N. Marzari and M. Fornari, *Phys. Rev. B* **81** 045204 (2010).

¹⁰ L. Hammersmidt, S. Schlecht and B. Paulus, *Phys. Stat. Sol. A* **210** 131-139 (2013).
¹¹ X. Shi, W. Zhang, L. D. Chen and J. Yang, *Phys. Rev. Lett.* **95** 185503 (2005).
¹² T. B. Massalski, H. Okamoto, P. R. Subramanian, and L. Kacpruk Eds., *Binary Alloy Phase Diagrams* 2nd Ed. (ASM International: Metals Park, OH, USA, vol. 2 1990), pp. 2664-2665.
¹³ M. D. Hornbostel, E. J. Hyer, J. Thiel, and D. C. Johnson, *J. Am. Chem. Soc.* **119**, 2665-2668 (1997).
¹⁴ A. Möchel, I. Sergueev, N. Nguyen, G. J. Long, F. Grandjean, D. C. Johnson, and R. P. Hermann, *Phys. Rev. B* **84**, 064302 (2011).
¹⁵ P. E. Blöchl, *Phys. Rev. B*, **50**, 17953 (1994).
¹⁶ G. Kresse and J. Furthmüller, *Phys. Rev. B*, **54**, 11169 (1996).
¹⁷ G. Kresse and D. Joubert, *Phys. Rev. B*, **59**, 1758 (1999).
¹⁸ J. P. Perdew, K. Burke, and M. Ernzerhof, *Phys. Rev. Lett.*, **77**, 3865 (1996).

- ¹⁹ H. J. Monkhorst and J. D. Pack, Phys. Rev. B, **13**, 5188 (1976).
- ²⁰ H. Ebert, D. Ködderitzsch and J. Minar, Rep. Prog. Phys. **74** 096501 (2010).
- ²¹ B. Skubic, J. Hellsvik, L. Nordström and O. Eriksson, J. Phys: Condens: Matter **20** 315203 (2008).
- ²² A. Togo, F. Oba and I. Tanaka, Phys. Rev. B **78**, 134106 (2008).
- ²³ T. Schmidt, G. Kliche, and H. D. Lutz, Acta Cryst. C **43**, 1678 (1987).
- ²⁴ L. Bergqvist, M. Råsander and A. Delin, in preparation (2014).
- ²⁵ E. S. Toberer, A. Zevalkink and G. J. Snyder, J. Mater. Chem. **21**, 15843 (2011).
- ²⁶ Y. Le Page and P. Saxe, Phys. Rev. B **65** 104104 (2002).
- ²⁷ X. Wu, D. Vanderbilt and D. R. Hamann, Phys. Rev. B **72** 035105 (2005).
- ²⁸ O. Hellman, I. A. Abrikosov and S. I. Simak, Phys. Rev. B **84** 180301 (2011).
- ²⁹ P. Souvatzis, O. Eriksson, M. I. Katsnelson and S. P. Rudin, Phys. Rev. Lett. **100**, 095901 (2008).